On the Mechanical Interactions in Suspension Rope – Sheave / Pulley Systems

Stefan Kaczmarczyk

Faculty of Arts, Science and Technology, The University of Northampton, UK

Keywords: suspension rope, bending stress, tensile stress, Euler-Bernoulli beam.

Abstract. Steel wire ropes employed as suspension means in lift systems are subjected to bending when passing around rigid traction sheaves/pulleys. In this paper, a suspension rope is represented as a moving Euler-Bernoulli beam and its global mechanical behaviour and interactions at the contact area are described by a nonlinear Boundary Value Problem with an unknown boundary. The problem is solved numerically for a lift system with the car suspension in a 2:1 roping configuration. The solution yields the curvature values, slope angles and the distribution of tensile and bending stresses along the rope span. It is demonstrated that the boundary angles vary during the lift travel and the distribution of stresses over the transition arc is nonuniform.

1 INTRODUCTION

Steel wire ropes (SWRs) and coated steel belts are used as suspension means in lift systems. The traction between the sheave and the suspension ropes is the fundamental consideration in the design of a traction lift installation [1]. Wire ropes have a finite life and are subject to the continual process of degradation associated with their operational conditions and stress fluctuations [2]. One of the primary mechanisms responsible for stress fluctuations is bending when the rope passes over the sheaves and pulleys. Consider the diagram shown in Fig. 1. The curvature of the suspension rope/belt increases along the rope from the point of application of tension T to the point of contact C where the curvature of the rope matches the curvature 1/R of the sheave/pulley surface. To meet the safety code requirements of BS EN81-20 the design must ensure that the ratio between the pitch diameter of sheaves and pulleys (or drums) and the nominal diameter of the suspension ropes shall be at least 40, regardless of the number of strands of the suspension ropes [3]. The suspension ropes must also meet BS EN 12385 – 5 [4] tensile strength grade requirements.

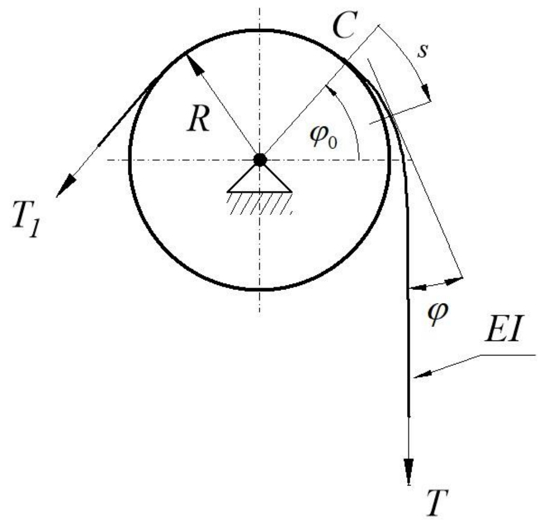

Figure 1 Rope passing over a sheave/pulley

2 EULER-BERNOULLI BEAM FORMULATION AND GLOBAL ROPE STRESSES

To determine the bending curvature, the rope can be considered as an elastic continuum and represented by a tensioned Euler-Bernoulli beam model [5]. The relationship between the bending moment M at the cross-section defined by the arc length s and the curvature κ is given by Eq. 1.

$$\kappa = \frac{M}{EI} \tag{1}$$

where EI is the bending stiffness of the rope. The curvature is equal to the reciprocal of the radius of curvature ρ and can be expressed as the rate of change of the slope angle φ along the rope arc as

$$\kappa = \frac{1}{\rho} = \frac{d\varphi}{ds} \tag{2}$$

Considering Eq. 1 and Eq. 2 the slope angle φ can be determined by solving the Boundary Value Problem (BVP) represented by the differential equation and boundary conditions defined by Eq. 3.

$$\begin{aligned} &\varphi'' - \beta^2 \sin\varphi = 0 \\ &\varphi'(0) = \kappa_0,\ \varphi'(\widehat{L}) = \kappa_{\widehat{L}} \end{aligned} \tag{3}$$

where $\beta^2 = \dfrac{T}{EI}$ and $(\ )'$ denotes differentiation with respect to s, $0 \le s \le \widehat{L}$, with $\widehat{L}$ representing the overall arc length of the rope. For small slope angles, the approximation $\sin\varphi \approx \varphi$ can be applied. Eq. 3 is then solved exactly to give the slope angle and the curvature as

$$\begin{aligned} &\varphi = C_1 e^{\beta s} + C_2 e^{-\beta s} \\ &\kappa = \varphi' = C_1 \beta e^{\beta s} - C_2 \beta e^{-\beta s} \end{aligned} \tag{4}$$

where C_1 and C_2 are constants to be determined from the boundary conditions at $s = 0$, $s = \widehat{L}$, respectively. It should be noted that the solution of Eq. 4 assumes that bending stiffness EI of the rope is constant. Once the Boundary Value Problem (3) is solved, the global bending stress in a wire of diameter d_w in the rope can be calculated by the following equation

$$\sigma_b = E\kappa \frac{d_w}{2} \tag{5}$$

where E represents the modulus of elasticity of the wire. It should be noted that this calculation provides an estimated global stress value (as first proposed by Reuleaux [6]) and assumes that the wire in the rope does not have a helix form. For a constant strand lay angle the real bending stresses in wires can be assumed to be the same as those given by Eq. 5 [6].

On the other hand, the global tensile stress in the wire rope can be calculated as

$$\sigma_t = \frac{T}{A} \tag{6}$$

where A is the global metallic cross-section area, determined as the sum of the cross-sections of all wires in the rope. While the real wire tensile stresses are larger than the global stress [6], Eq. 6 presents a useful practical estimation of the rope tensile stress conditions.

3 MOVING ROPE MODEL

For a rope–sheave/pulley system in motion the BVP (3) needs to be developed further. Fig. 2 shows a free body diagram of the rope segment of length ds. The equilibrium of forces in the normal direction and the tangential direction, respectively, yields the following equations of motion [5]

$$\begin{aligned} &\kappa'' - \frac{1}{EI}\left(T - mv^2\right)\kappa + \frac{mg}{EI}\sin\varphi = 0 \\ &T' - mvv' + EI\kappa\kappa' + mg\cos\varphi = 0 \end{aligned} \tag{7}$$

where g is the acceleration of gravity, v is the axial speed and m is the mass per unit length of the rope.

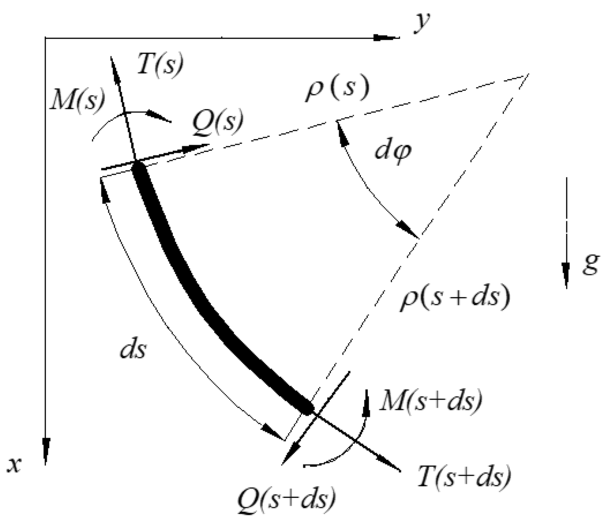

Figure 2 Free body diagram of the rope segment

By considering that the Cartesian coordinates of rope sections are expressed as

$$\frac{dx}{ds} = \cos\varphi$$
$$\frac{dy}{ds} = \sin\varphi$$
(8)

The model given in terms of Eq. 7 and Eq. 8 can be formulated as a 1st order system defined by

$$\mathbf{y}' = \mathbf{f}\left(s, \mathbf{y}; t\right), \quad 0 \le s \le \widehat{L}(t) \tag{9}$$

where t denotes time and

$$\begin{aligned} &\mathbf{y} = \left[\kappa, \kappa', T, \widehat{L}, \varphi, x, y\right]^T \\ &\mathbf{f} = \left[\kappa', \quad \frac{1}{EI}\left(T - mv^2\right)\kappa - \frac{mg}{EI}\sin\varphi, \quad mvv' - EI\kappa\kappa' - mg\cos\varphi, \quad 0, \quad \kappa, \quad \cos\varphi, \quad \sin\varphi\right]^T \end{aligned} \tag{10}$$

It should be noted that vector **y** represents unknown quantities and includes the arc length $\widehat{L}(t)$ which is an unknown boundary.

4 THE SOLUTION STRATEGY AND A LIFT SYSTEM EXAMPLE

To solve the equation system (9) the boundary conditions need to be defined. For example, consider a lift system with the suspension ropes at the car side in a 2:1 roping configuration (see Fig. 3). By taking into account the suspension rope span between points A and B, the boundary conditions are defined in Eq. 11.

$$\begin{aligned}&\kappa(0)=-\frac{1}{R},\ \kappa(\widehat{L})=-\frac{1}{r},\ T(\widehat{L})=\frac{Mg}{2n_{SR}\cos\varphi(\widehat{L})},\ x(0)=-R\sin\varphi(0),\ y(0)=R\cos\varphi(0),\\&x(\widehat{L})=L-r\sin\varphi(\widehat{L}),\ y(\widehat{L})=R-r\left[1-\cos\varphi(\widehat{L})\right]\end{aligned} \tag{11}$$

where n_{SR} is the number of ropes. The solution strategy for the BVP (9-11) with the unknown time-varying boundary $\widehat{L}(t)$ involves reformulation into the 'standard' form defined over a fixed interval [7]. This is accomplished by introducing nondimensional variables defined by Eq. 12.

$$\tilde{s}=\frac{s}{\widehat{L}},\quad \tilde{x}=\frac{x}{\widehat{L}},\quad \tilde{y}=\frac{y}{\widehat{L}},\quad \tilde{\kappa}=\widehat{L}\kappa,\quad \tilde{T}=\frac{T\widehat{L}^2}{EI},\ \tilde{v}=\frac{v}{c_0} \tag{12}$$

where $c_0=\sqrt{\dfrac{Mg}{n_{SR}m}}$. The system (9-11) can then be expressed in terms of variables (12) (see Appendix) and solved numerically by the application of a collocation method for BVPs. The solution procedure involves providing the initial solution guess. For the guess, the estimations given by Eq. (4) are used and the problem is solved in MATLAB with the **bvp4c** function [8].

Table 1 Fundamental parameters

Parameter	Value	Unit
M	1800	kg
n_{SR}	4	
m	0.407	kg/m
A	42.5	mm^2
d_w	1	mm
EI	1.6	Nm^2
V	1.5	m/s
$L(0)$	2	m
R	0.28	m
r	0.25	m

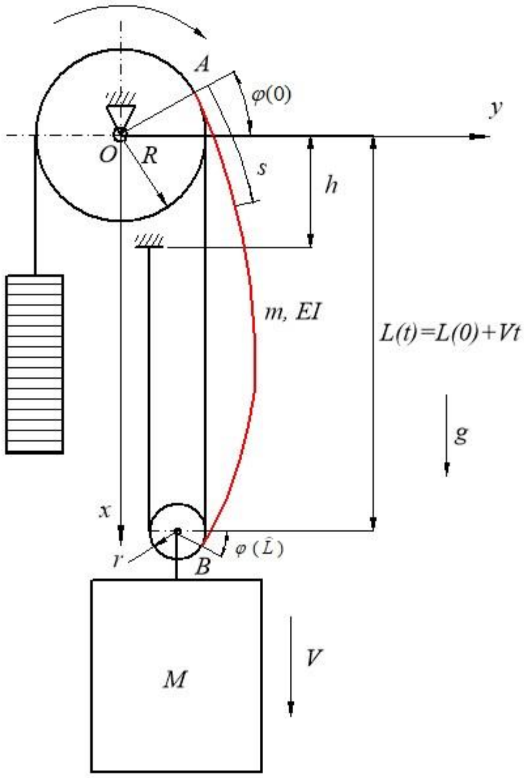

Figure 3 Lift system

5 NUMERICAL RESULTS

The system parameters used in the numerical simulations are presented in Table 1. The suspension rope is an 11 mm 8×19 S - FC rope [9], and the *EI* value is determined by laboratory vibration tests. The simulation is carried out for the lift moving down at constant speed over the time interval 0 – 5 s. Fig. 4 shows the variation of slope angles during the lift travel, determined at the contact points at $s=0$ and at $s=\widehat{L}$, respectively. The variation is small, and the plots demonstrate slightly larger values at the car pulley. The curvature changes and global bending stresses (calculated from Eq. 5) over the rope span length are illustrated in Fig. 5(a) and Fig. 5(b), respectively. Fig. 6 shows the variation of global tensile stresses (determined from Eq. 6).

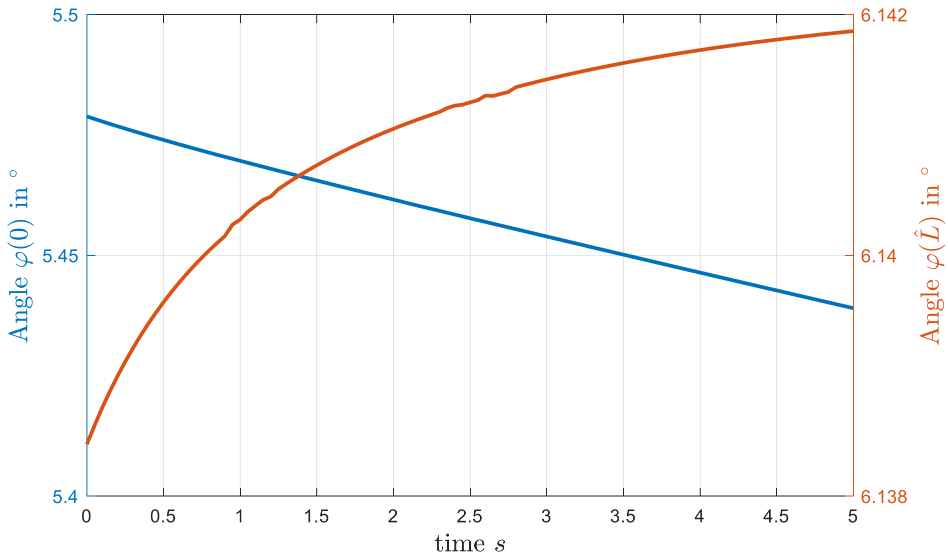

Figure 4 The slope angle at the boundary points: $s=0$ and $s=\widehat{L}$

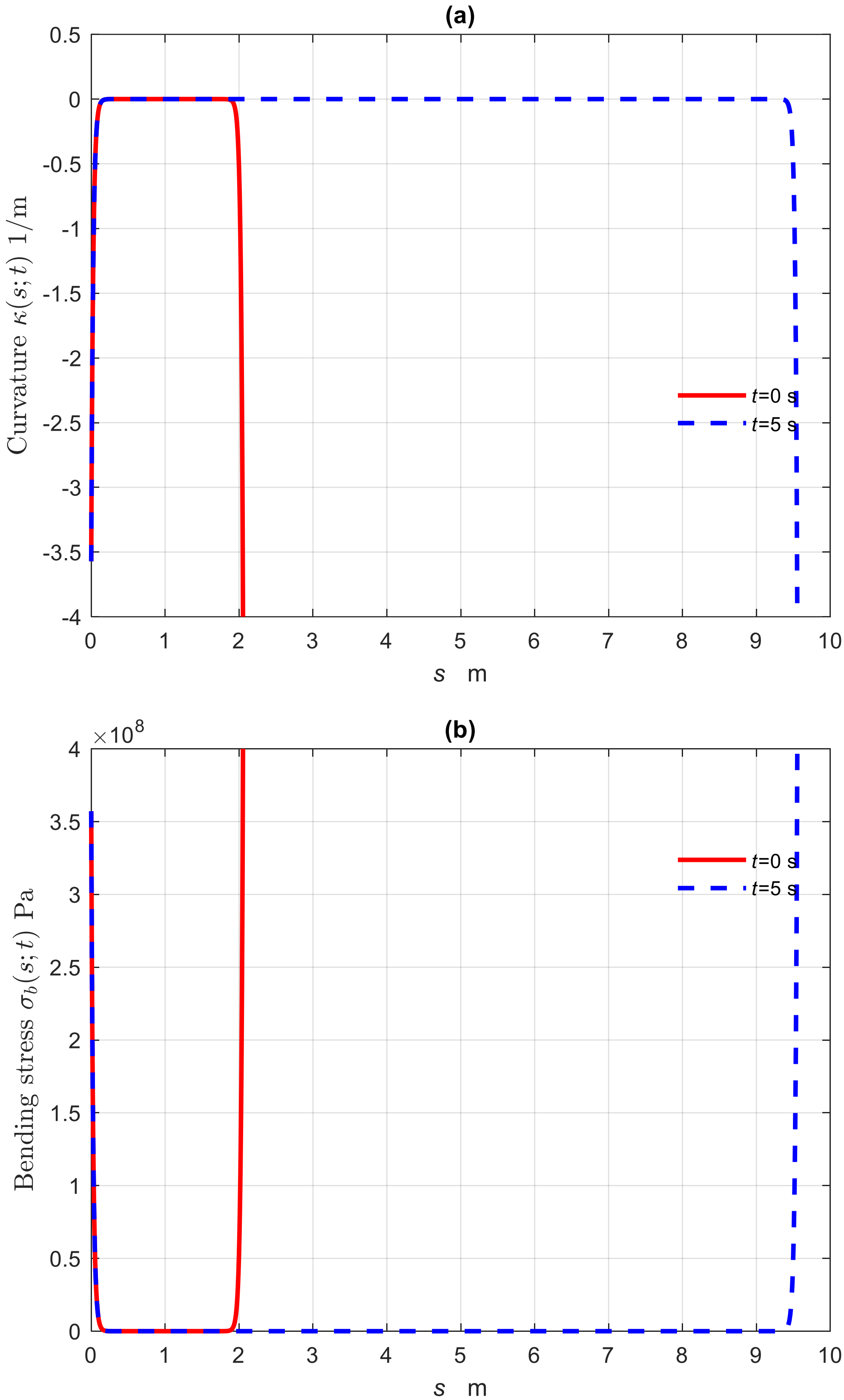

Figure 5 (a) curvatures and (b) bending stresses

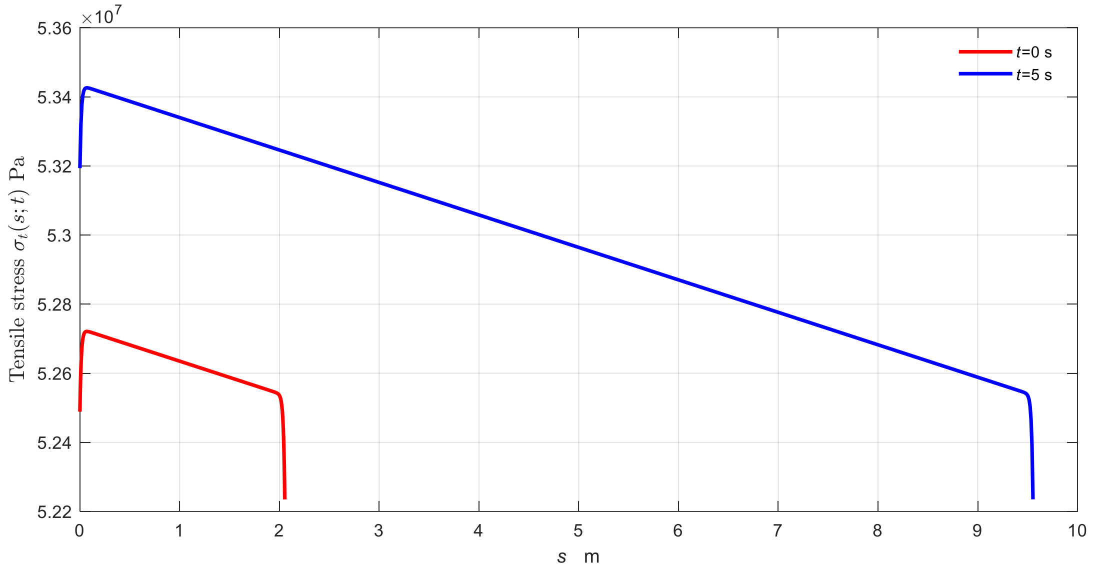

Figure 6 Tensile stresses

6 SUMMARY AND CONCLUSIONS

The work presented in this paper demonstrates a simplified model to analyse the global behaviour of lift SWR suspension ropes passing over a traction sheave/pulley system. The model is used to calculate fundamental parameters describing the performance of the ropes subjected to bending and tensile stresses. The method is based on the application of a tensioned Euler-Bernoulli beam which results in a nonlinear BVP problem. The problem can be treated by standard ODE solvers. The results show estimated bending and tensile stresses that vary along the rope length. The bending stresses can be reduced by using smaller diameter ratios between the pitch diameter of sheaves/pulleys and the nominal diameter of the suspension ropes. The lifetime/endurance of SWRs running over sheaves/pulleys can then be estimated in terms of the number of bending cycles until breakage [10].

REFERENCES

[1] J.P. Andrew and S. Kaczmarczyk, *Systems Engineering of Elevators*. Elevator World, Mobile, AL (2011).

[2] C.R. Chaplin, "Interactive Fatigue in Wire Rope Applications". In the *Proceedings of Mechanics of Slender Structures,* 23-25 July 2008, University of Maryland Baltimore County, USA.

[3] British Standards Institute, *Safety rules for the construction and installation of lifts — Lifts for the transport of persons and goods Part 20: Passenger and goods passenger lifts.* BS EN 81-20:2020.

[4] British Standards Institute, *Steel wire ropes — Safety Part 5: Stranded ropes for lifts.* BS EN 12385-5:2002.

[5] S. Kaczmarczyk and S. Mirhadizadeh, Quasi-stationary mechanics of elastic continua with bending stiffness wrapping on a pulley system. *Journal of Physics: Conference Series*, 2016, Vol. 721, 012011 DOI 10.1088/1742-6596/721/1/012011.

[6] K. Feyrer, *Wire Ropes*. Springer-Verlag Berlin Heidelberg (2015).

[7] U. Ascher and R.D. Russell, Reformulation of boundary value problems into "standard" form. *SIAM Review,* 1981, Vol. 23(2), pp. 2398-254.

[8] J. Kierzenka Tutorial on solving BVPs with BVP4C. MATLAB Central File Exchange https://www.mathworks.com/matlabcentral/fileexchange/3819-tutorial-on-solving-bvps-with-bvp4c (Accessed 29 May 2023)

[9] Pfeifer DRAKO *Elevator Products* *https://www.pfeifer.info/out/assets/PFEIFER-DRAKO_ELEVATOR-PRODUCTS_BROCHURE_EN.PDF* (Accessed 28 May 2023).

[10] W. Vogel, Influences on lifetime of wire ropes in traction lifts. *Journal of Physics: Conference Series*, 2016, Vol. 721, 012014 DOI 10.1088/1742-6596/721/1/012014.

APPENDIX

Substituting the nondimensional parameters Eq. 12 into Eq. 7 yields [5]

$$\begin{aligned} &\tilde{\kappa}'' - \left(\tilde{T} - \beta^2 \hat{L}^2 \tilde{v}^2\right)\tilde{\kappa} + \frac{mg}{EI}\hat{L}^3 \sin\varphi = 0 \\ &\tilde{T}' - \beta^2 \hat{L}^2 \tilde{v}\tilde{v}' + \tilde{\kappa}\tilde{\kappa}' + \frac{mg}{EI}\hat{L}^3 \cos\varphi = 0 \end{aligned} \tag{A1}$$

where $\beta = \sqrt{\dfrac{Mg}{n_{SR} EI}}$ and $(\ )'$ denotes now differentiation with respect to the nondimensional variable $\tilde{s}$ defined over the fixed interval $0 \le \tilde{s} \le 1$. Eq. 10 assumes then the following form:

$$\begin{aligned} &\mathbf{y} = \left[\tilde{\kappa}, \tilde{\kappa}', \tilde{T}, \hat{L}, \varphi, \tilde{x}, \tilde{y}\right]^T \\ &\mathbf{f} = \left[\tilde{\kappa}', \quad \left(\tilde{T} - \beta^2 \hat{L}^2 \tilde{v}^2\right)\tilde{\kappa} - \frac{mg}{EI}\hat{L}^3 \sin\varphi, \quad \beta^2 \hat{L}^2 \tilde{v}\tilde{v}' + \tilde{\kappa}\tilde{\kappa}' - \frac{mg}{EI}\hat{L}^3 \cos\varphi, \quad 0, \quad \tilde{\kappa}, \quad \cos\varphi, \quad \sin\varphi\right]^T \end{aligned} \tag{A2}$$

BIOGRAPHICAL DETAILS

Dr Stefan Kaczmarczyk is Professor of Applied Mechanics and Postgraduate Programme Leader for Lift Engineering at the University of Northampton, UK. His expertise is in applied dynamics and vibration, computer modelling and simulation with applications to vertical transportation and material handling systems. He has published over 100 journal and international conference papers in this field. He is a Chartered Engineer, elected Fellow of the Institution of Mechanical Engineers and a Fellow of the Higher Education Academy.